Phonon thermal conductivity of bismuth alloys

V. D. Kagan and N. A. Red'ko

A. F. Ioffe Physicotechnical Institute, Academy of Sciences of the USSR, Leningrad

(Submitted 17 September 1990)
Zh. Eksp. Teor. Fiz. **100**, 1205–1218 (October 1991)

The phonon thermal conductivity $\varkappa_{\rm ph}$ of alloys $\mathrm{Bi}_{1-x}\mathrm{Sb}_x$ ($0 \leqslant x \leqslant 0.16$) has been studied as a function of the antimony concentration and the temperature ($1.8 \leqslant T \leqslant 300$ K). The temperature dependence has been observed for the phonon thermal conductivity for $\mathrm{Bi}_{1-x}\mathrm{Sb}_x$ alloys of various compositions, for the first time. For the "clean" insulator the behavior is $\varkappa_{\rm ph}(T) \propto \exp(\theta/bT)$ for $T < \theta$ and $\varkappa_{\rm ph}(T) \propto T^{-1}$ for $T > \theta$. This behavior is characteristic of pure bismuth ($x = 0$), which consists of only a single isotope. The behavior found for the "dirty" insulator is $\varkappa_{\rm ph}(C,T) \propto C^{-2/3}T^{-4/3}$ for $T < \theta$ and $\varkappa_{\rm ph}(T) \propto C^{-2/3}T^{-1/3}$ for $T > \theta$. This behavior was found for the alloy $\mathrm{Bi}_{1-x}\mathrm{Sb}_x$ ($0.08 < x \leqslant 0.16$). Here $\theta \approx 120$ K is the Debye temperature for Bi, and C is the concentration of local defects which arise because of the difference between the relative atomic masses of Bi and Sb. According to a theoretical analysis, the behavior of the phonon thermal conductivity observed experimentally as a function of the temperature and the defect concentration is typical of a dirty insulator. It arises because of a composite mechanism involving scattering of the phonons by both defects and phonons, but Simons processes are predominant in the phonon-phonon interaction.

INTRODUCTION

Bismuth is an excellent model substance for a study of the phonon thermal conductivity. In the first place, bismuth consists of only a single isotope, so there is no isotopic scattering for phonons. That scattering causes a serious limitation on the thermal conductivity in solids at low temperatures and makes it impossible to determine the behavior in different regimes of the flow of the phonon gas.

Second, in the case of bismuth a method is available for growing high-quality single crystals of large dimensions.

Third, in the compensated semimetal Bi, with a charge-carrier density $n = p \approx 3 \cdot 10^{17}$ cm^{-3}, at low temperatures ($2 < T < 20$ K), the heat is transferred primarily by phonons.[1,2] The scattering of phonons by charge carriers for $T > 2$ K is negligible.[3] The phonon thermal conductivity $\varkappa_{\rm ph}$ in a high-quality bulk bismuth crystal (8.8×8.6 mm^2) reaches a maximum (and record high) value of 86 W/(cm·K) at a temperature $T_M \approx 3.5$ K (Ref. 1). The primary reason for the scattering of phonons by phonons is the anharmonicity of the lattice vibrations of Bi, which leads to a characteristic Peierls dependence for the phonon thermal conductivity, which was observed in the experiments of Refs. 1 and 3: $\varkappa_{\rm ph}(T) \propto \exp(\theta/bT)$ for $T_M < T < \theta$ and $\varkappa_{\rm ph}(T) \propto T^{-1}$ for $T > \theta$, where $\theta \approx 120$ K is the Debye temperature for Bi. In bismuth, the temperature dependence of the mean free path of the phonons involved in the N and U processes at low temperatures has been found from the experimental data, including data on the thermal conductivity: l_U (cm) $= \tau_U \bar{s} \approx 5 \cdot 10^5 \exp(40/T)$ (Ref. 3), l_N (cm) $= \tau_N \bar{s} \approx AT^{-4}$, where $A \approx 0.4$ and 3 (Refs. 4 and 5), and $\bar{s} = 1.5 \cdot 10^5$ cm/s is the average sound velocity.

Fourth, bismuth can be used to form binary alloys, and alloys of various compositions can be used to study the temperature dependence of the phonon thermal conductivity. The antimony atoms in the Bi–Sb alloys occupy sites of the Bi crystal lattice. For phonons, they constitute scattering centers similar to isotopic scattering centers (the atomic masses of Bi and Sb differ by a factor of 1.7).

The temperature dependence of the phonon thermal conductivity of Si–Sb alloys has been the subject of several studies,[6-8] but the measurements of $\varkappa_{\rm ph}$ in Refs. 7 and 8 were restricted to the narrow temperature interval $T < 40$ K. In studies in which the thermal conductivity has been measured at temperatures above 20 K, the phonon and electron components have not been distinguished. Only the total thermal conductivity has been studied (this is true of Ref. 6, for example). The results of a study of the total thermal conductivity of Bi–Sb alloys at temperatures over the range 77–300 K were reported in Ref. 6, and it was concluded that the electron component is a major component of the thermal conductivity. The phonon thermal conductivity of $\mathrm{Bi}_{1-x}\mathrm{Sb}_x$ ($0 < x < 0.2$) alloys was studied in Ref. 7 over the temperature interval 5–40 K. It was found that there is a significant decrease in the thermal conductivity with increasing antimony concentration. The analysis of the experimental data on the thermal conductivity of Bi–Sb alloys which was carried out in Ref. 7 and the conclusion, based on that analysis, that the dominant scattering of phonons by internal boundaries is due to composition fluctuations in the alloys do not agree with the results of other studies. For example, a study[8] in which one of the present authors participated yielded data showing a significant size effect of the phonon thermal conductivity at low temperatures in the alloy $\mathrm{Bi}_{0.88}\mathrm{Sb}_{0.12}$.

The research which was been carried out on the temperature dependence of the phonon thermal conductivity of $\mathrm{Bi}_{1-x}\mathrm{Sb}_x$ alloys for $T < 20$ K is incomplete. At temperatures above 20 K, there are no data in the literature on the phonon thermal conductivity or on its dependence on the temperature or the composition of the alloy.

In the present paper we are reporting an analysis of our measurements of the temperature dependence of the phonon thermal conductivity of $\mathrm{Bi}_{1-x}\mathrm{Sb}_x$ ($0 \leqslant x \leqslant 0.16$) alloys of various compositions over the temperature range $1.8 \leqslant T \leqslant 300$ K. Preliminary experimental results on the thermal conductivity of Bi–Sb alloys were published in Ref. 9.

0038-5646/91/100664-08$03.00

EXPERIMENTAL RESULTS

1. The $Bi_{1-x}Sb_x$ alloys consist of the elements Bi and Sb, which belong to group V and which differ in atomic mass ($m_{Bi} \approx 209$, $m_{Sb} \approx 122$) and also ionic radius ($r_{Bi} \approx 0.62$ Å, $r_{Sb} \approx 0.74$ Å). The differences in the atomic properties of Bi and Sb lead to the formation of local defects at antimony-atom sites in the crystal lattice of the Bi–Sb alloy. The presence of local defects in the Bi–Sb lattice gives rise to intense scattering (similar to isotopic scattering) of phonons by these defects, and it makes possible an experimental study of the effect of the number of defects (the Sb concentration) in the alloy on the magnitude and temperature dependence of the phonon thermal conductivity.

The bismuth and antimony atoms in the Bi–Sb lattice differ in force constants as well as atomic masses. As a result, the lattice constant depends on the antimony concentration in the alloy.[10] There is also a change in the energy spectrum of the charge carriers in the $Bi_{1-x}Sb_x$ alloys as their composition is varied, from a semimetallic state ($0 \leqslant x \leqslant 0.07$) to a semiconducting state ($0.07 < x < 0.22$).[11] Bismuth is a compensated semimetal with a carrier density $n = p \approx 3 \cdot 10^{17}$ cm^{-3}, and in the $Bi_{1-x}Sb_x$ alloys with $0 \leqslant x < 0.07$ the carrier density decreases with increasing antimony concentration.[11]

In pure bismuth[1,2] and in Bi–Sb alloys[8] the heat is transferred primarily by phonons over the temperature interval $2 < T < 20$ K, while at $T > 20$ K electrons come into play along with the phonons. The electron component increases with the temperature, and at $T \geqslant \theta \approx 120$ K the electron and phonon components are comparable in magnitude. These conclusions follow from the results of the present study. The presence of carriers in Bi does not result in significant scattering of phonons by electrons for $T > 2$ K (Ref. 3); the same comment applies, even more strongly, to $Bi_{1-x}Sb_x$ ($0 < x < 0.07$) alloys, for which the carrier density is lower than in Bi.

This analysis leads us to the conclusion that a fairly intense scattering of phonons by defects comes into play along with the phonon-phonon scattering in Bi–Sb alloys. The phonon-phonon scattering is observed in bismuth at temperatures below and above the Debye temperature.

2. To measure the thermal conductivity of the $Bi_{1-x}Sb_x$ alloys, we used samples which were rectangular parallelepipeds. The long dimension of the samples coincided with the bisector of the angle between the C_1 axis and the direction of the heat flux, in other words, with ∇T. The samples were cut by electron discharge machining from single-crystal bars grown by horizontal zone refining. After the cutting, the samples were etched in a 1:1 C_2H_5OH–HNO_3 solution. The transverse dimensions of the samples were chosen so that the size effect would not affect the phonon thermal conductivity $\varkappa_{ph}$ for $T > T_M$. The samples thus had dimensions of approximately $4 \times 4 \times 40$ mm^3.

The magnitude of the thermal conductivity was determined by the method of steady-state heat flux through the sample. The sample was soldered to the bottom of a vacuum chamber immersed in a temperature-regulation liquid (nitrogen, hydrogen, or helium). Carbon resistance thermometers were used over the range 1.4–60 K, and copper-constantan thermocouples were used for $T > 40$ K.

The phonon component of the thermal conductivity, $\varkappa_{22}$ (∇T is directed along the C_1 axis) was distinguished by applying a classically strong magnetic field to suppress the electron component of the thermal conductivity.

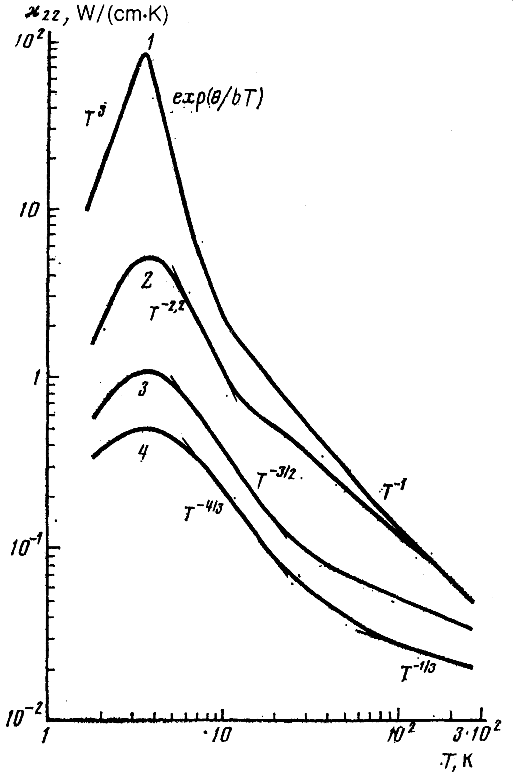

FIG. 1. Temperature dependence of the phonon thermal conductivity, $\varkappa_{22}(T)$, of single-crystal samples of bismuth-based alloys ($\nabla T \| C_i$). *1*—Pure bismuth;[1] *2–4*—$Bi_{1-x}Sb_x$ alloys; *2*—$x = 0.001$; *3*—0.03; *4*—0.13.

3. Figure 1 shows the typical temperature dependence $\varkappa_{ph}(T)$ for the alloys $Bi_{1-x}Sb_x$ ($0 \leqslant x \leqslant 0.16$) of various compositions. As we mentioned earlier, bulk samples were used for measurements of the thermal conductivity of the Bi–Sb alloys, so the transverse dimensions of the sample did not affect the temperature dependence of the thermal conductivity at $T_M < T < \theta$. With increasing Sb concentration in the Bi–Sb alloys, the phonon thermal conductivity becomes smaller than $\varkappa_{ph}$ of pure Bi over the entire temperature range studied, $1.8 \leqslant T \leqslant 300$ K. The effect is particularly noticeable at Sb concentrations above 0.1 at. %.

The temperature dependence of the phonon thermal conductivity of bismuth is exponential for $T_M < T < 10$ K, while it is a power law in the Bi–Sb alloys. While for Bi at $T > \theta$ we have $\varkappa_{ph}(T) \propto T^{-1}$, for a Bi–Sb alloy we have $\varkappa_{ph}(T) \propto T^{-n}$, where $n \leqslant 1$. The deviation of the temperature dependence of the phonon thermal conductivity of the $Bi_{1-x}Sb_x$ alloys from the $\varkappa_{ph}(T) \propto T^{-1}$ law sets in at a threshold Sb concentration $x \geqslant 0.003$, while there is no such threshold antimony concentration near the temperature of the maximum in the phonon thermal conductivity of Bi–Sb alloys. The thermal conductivity decreases at an arbitrarily low Sb concentration. Near the maximum of the thermal conductivity of the alloys, the defects have a far greater effect on the thermal conductivity than at higher temperatures. For example, the magnitude of the phonon thermal conductivity of the alloy $Bi_{0.87}Sb_{0.13}$ is lower than $\varkappa_{ph}$ of pure Bi at $T = 300$ K by a factor of more than 2. At

$T=\theta\approx 120$ K, it is smaller by a factor ~ 4; near the maximum of the thermal conductivity at $T\approx 4$ K it is smaller by more than two orders of magnitude.

The temperature (T_M) at which the thermal conductivity reaches its maximum for the alloys studied does not shift as the Sb concentration is raised to 16 at. %. It lies near $T=4$ K and is fairly close to the value $T_M\approx 3.5$ K for pure Bi (curves *1-4* in Fig. 1). The peak on the $\varkappa_{\mathrm{ph}}(T)$ curve, however, becomes more rounded as the Sb concentration is raised. This can be seen from the change in the temperature dependence of the thermal conductivity at $T=2$ K of the alloys $\mathrm{Bi}_{1-x}\mathrm{Sb}_x$ as their composition is varied: $\varkappa_{\mathrm{ph}}(T)\propto T^{2.5}$ for $\mathrm{Bi}_{0.999}\mathrm{Sb}_{0.001}$, $\varkappa_{\mathrm{ph}}(T)\propto T^{0.9}$ for $\mathrm{Bi}_{0.87}\mathrm{Sb}_{0.13}$, and $\varkappa_{\mathrm{ph}}(T)\propto T^3$ for pure Bi.

The power-law dependence $\varkappa_{\mathrm{ph}}(T)$ at temperatures below and above the Debye temperature is different for alloys of different compositions. For example, we find $\varkappa_{\mathrm{ph}}(T)\propto T^{-2.2}$ for $\mathrm{Bi}_{0.999}\mathrm{Sb}_{0.001}$ for $T_M<T<10$ K, while for $T\geqslant\theta$ we find $\varkappa_{\mathrm{ph}}(T)\propto T^{-1}$ (curve *2* in Fig. 1). For the alloys $\mathrm{Bi}_{1-x}\mathrm{Sb}_x$ $(0.03\leqslant x<0.08)$ for $T_M<T<20$ K we have $\varkappa_{\mathrm{ph}}(T)\propto T^{-3/2}$, while for $T\geqslant\theta$ we have $\varkappa_{\mathrm{ph}}(T)\propto T^{-1/2}$ (curve *3* in Fig. 1). For alloys $\mathrm{Bi}_{1-x}\mathrm{Sb}_x$ $(0.08<x\leqslant 0.16)$ we have $\varkappa_{\mathrm{ph}}(T)\propto T^{-4/3}$ for $T_M<T<20$ K and $\varkappa_{\mathrm{ph}}(T)\propto T^{-1/3}$ for $T\geqslant\theta$ (curve *4* in Fig. 1).

Figure 2 shows $\varkappa_{\mathrm{ph}}$ of the $\mathrm{Bi}_{1-x}\mathrm{Sb}_x$ $(0\leqslant x\leqslant 0.16)$ alloys at $T=10$ K versus the concentration of local defects, C, defined as the mean square relative fluctuation of the mass of the Bi and Sb atoms at lattice sites:

$$C=\overline{\Delta m^2}/(\bar{m})^2=(m_{\mathrm{Bi}}-m_{\mathrm{Sb}})^2x(1-x)/[m_{\mathrm{Sb}}x+m_{\mathrm{Bi}}(1+x)]^2,$$

where x is the relative antimony concentration. The curve of the phonon thermal conductivity of the $\mathrm{Bi}_{1-x}\mathrm{Sb}_x$ alloys as a function of the defect concentration shown in Fig. 2 corresponds to the hyperbolic law $\varkappa_{\mathrm{ph}}(C)\sim C^{-1/2}$ at low defect concentrations, $2\cdot 10^{-3}<C<0.017$. This interval corresponds to antimony concentrations $0.01<x<0.1$. At high defect concentrations, $0.017<C<0.027$ $(0.1<x<0.16)$, the curve is described better by a $\varkappa_{\mathrm{ph}}(C)\propto C^{-2/3}$ law.

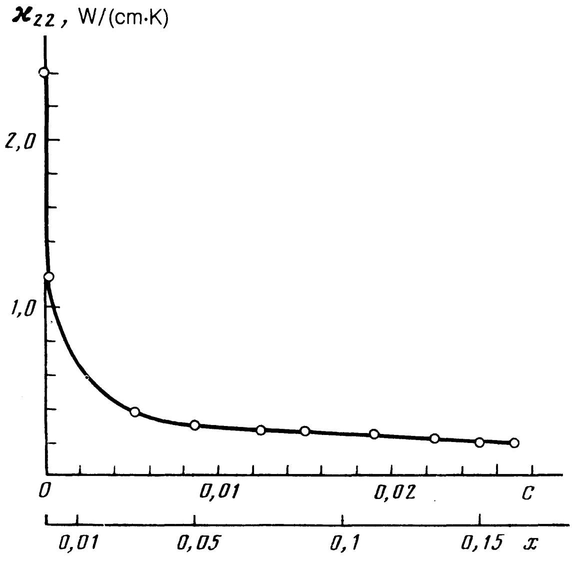

FIG. 2. Phonon thermal conductivity $\varkappa_{22}(C,x)$ of $\mathrm{Bi}_{1-x}\mathrm{Sb}_x$ $(0\leqslant x\leqslant 0.16)$ alloys at $T=10$ K as a function of the relative antimony concentration x and as a function of the local defect concentration C.

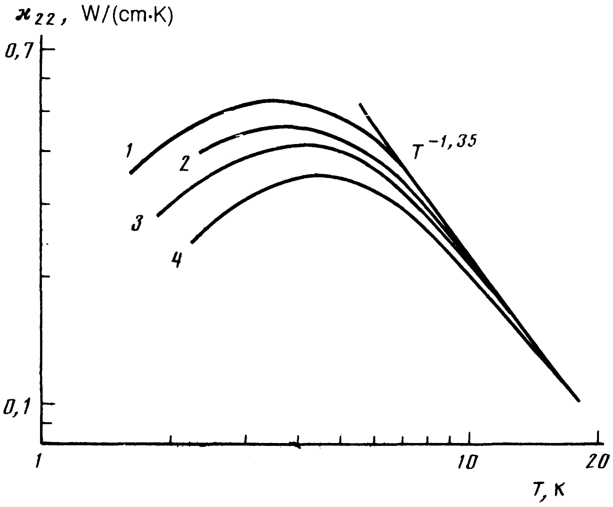

FIG. 3. Temperature dependence of the phonon thermal conductivity $\varkappa_{22}(\nabla T\|C_1)$ of a $\mathrm{Bi}_{0.88}\mathrm{Sb}_{0.12}$ alloy for samples with various transverse dimensions. *1*—$d_1\approx 3.18$ mm, $d_2\approx 3.3$ mm, $d=(d_1d_2)^{1/2}\approx 3.2$ mm; *2*—$d_1\approx 2.3$ mm, $d_2\approx 2.0$ mm, $d\approx 2.2$ mm; *3*—$d_1\approx 1.33$ mm, $d_2\approx 1.15$ mm, $d\approx 1.24$ mm; *4*—$d_1\approx 0.99$ mm, $d_2\approx 0.88$ mm, $d\approx 0.8$ mm.

Figure 3 shows the phonon thermal conductivity for the alloy $\mathrm{Bi}_{0.88}\mathrm{Sb}_{0.12}$ as a function of the temperature and the transverse dimensions of the test samples. The thermal conductivity at the maximum behaves in the following way as a function of the effective transverse dimension $d=(d_1d_2)^{1/2}$ of the $\mathrm{Bi}_{0.88}\mathrm{Sb}_{0.12}$ samples: $\varkappa_{\mathrm{ph}}(T_M)\propto d^{1/4}$, where d_1 and d_2

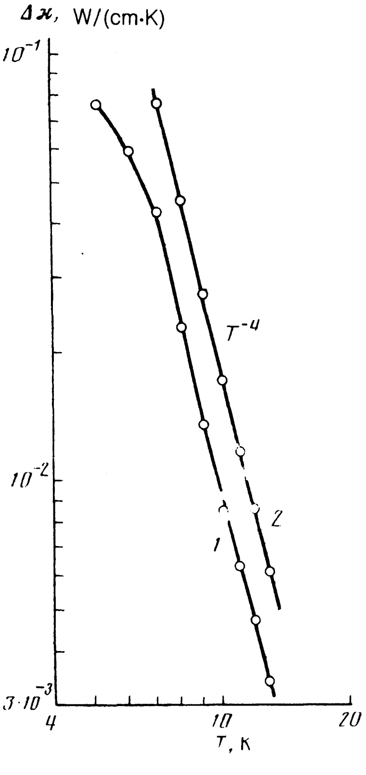

FIG. 4. Temperature dependence of the increment $\Delta\varkappa_i=\varkappa_0-\varkappa_i$ in the thermal conductivity for the alloy $\mathrm{Bi}_{0.88}\mathrm{Sb}_{0.12}$. *1*—$\Delta\varkappa_1=\varkappa_0-\varkappa_4$; *2*—$\Delta\varkappa_2=\varkappa_0-\varkappa_3$. Here $\varkappa_0=\varkappa_1$, $\varkappa_3$, and $\varkappa_4$ are the thermal conductivities of the alloy $\mathrm{Bi}_{0.88}\mathrm{Sb}_{0.12}$ according to measurements on samples 1, 3, and 4, as shown in Fig. 3 (the number of the sample is the same as the number of the curve in Fig. 3).

are the transverse dimensions of the sample. This behavior differs from that for pure bismuth, for which $\varkappa_{\rm ph}(T_M) \propto d$.

In the alloys, as in pure Bi (Ref. 3), we see a size effect in the thermal conductivity for $T > T_M$. This effect influences the temperature dependence of the thermal conductivity. In bulk samples of the alloy $Bi_{0.88}Sb_{0.12}$ we have $\varkappa_{\rm ph}(T) \propto T^{-n}$, where $n \approx 4/3$, while for samples with finite transverse dimensions we have $n < 4/3$. For a sample with $d = 0.88$ mm, for example, we find $\varkappa_{\rm ph}(T) \propto T^{-1/2}$ (Fig. 3). Because of the scattering of phonons by the surface of the sample, the thermal conductivity for $T > T_M$ is lower than that of a bulk sample, $\varkappa_0$, by an amount $\Delta\varkappa = \varkappa_0 - \varkappa$. In this case the sample with the largest transverse dimensions, $d \approx 3.3$ mm, is a bulk sample, and the temperature dependence for it is $\varkappa_0(T) \propto T^{-4/3}$.

Figure 4 shows the temperature dependence of the increment $\Delta\varkappa_i$ in the thermal conductivity because of the size effect for $Bi_{0.88}Sb_{0.12}$ samples 3 and 4. These are the samples which have the smallest effective transverse dimensions, $d = 0.88$ mm, and $d = 1.24$ mm (see Fig. 3 regarding the designations of the samples). The temperature dependence of the increment in the thermal conductivity is approximately $\Delta\varkappa \propto T^{-4}$.

To explain the observed behavior of the phonon thermal conductivity of the Bi–Sb alloys as a function of the temperature, the Sb concentration, and the transverse dimensions of the sample, we have carried out a theoretical analysis of the behavior of the thermal conductivity as a function of these parameters in dirty insulators. We turn now to that analysis.

THEORETICAL ANALYSIS OF THE THERMAL CONDUCTIVITY OF DIRTY INSULATORS

1. In the case of the isotropic Debye model we have the following expression for the thermal conductivity:

$$\varkappa = \frac{2}{3(2\pi)^2} \sum_i \int_0^{\theta/\hbar} d\omega \rho(\omega) s_i^2 \hbar\omega\tau_i \, \partial N_0^i / \partial T, \qquad (1)$$

$$\rho(\omega) = \omega^2/(\bar{s})^2, \quad N_0 = [\exp(\hbar\omega/T) - 1]^{-1},$$

where i is the index of the phonon branch, θ is the Debye temperature, s_i is the sound velocity, $\rho(\omega)$ is the density of phonon states, $\bar{s}$ is the average sound velocity, τ is the relaxation time, N_0 is the Planck distribution function, and T is the temperature in energy units. The relaxation time of the phonon distribution function is determined by scattering of phonons by impurities and by phonon-phonon scattering:

$$\tau^{-1} = \tau_I^{-1} + \tau_{\rm ph}^{-1}, \quad \tau_I^{-1} = A\omega^4\hbar^2/\theta^3, \qquad (2)$$

where the constant A is proportional to the concentration of impurity atoms, C.

In a dirty insulator, the scattering of thermal-energy phonons by impurity atoms (impurity scattering) is far stronger than the phonon-phonon scattering:

$$\tau_I(T)/\tau_{\rm ph}(T) \ll 1 \text{ for } T \ll \theta; \quad \tau_I(\theta)/\tau_{\rm ph}(\theta) \ll 1 \text{ for } T \gg \theta. \qquad (3)$$

Despite the strong dependence of the impurity scattering on the frequency, however, we cannot restrict expressions (1) and (2) to simply the impurity scattering. The integral would diverse at low frequencies. We must also retain the phonon-phonon relaxation, which has a weaker frequency dependence and thus makes it possible to eliminate the divergence of the integral at its lower limit. It follows that the integral (1) is dominated by those subthermal phonons for which the phonon-phonon scattering intensity is comparable to the intensity of the impurity scattering.

2. We first consider the contribution of transverse phonon branches to (1). For low-frequency phonons, the most important processes are the attachment of a subthermal transverse phonon (t) to a thermal longitudinal phonon (l), accompanied by the formation of a longitudinal thermal phonon (l), and the inverse decay process, i.e., Landau–Rumer processes:[12]

$$\begin{aligned} \tau_{\rm ph}^{-1} &= b_1\omega T^4/\rho(\bar{s})^2 s_l^3\hbar^3 \text{ for } T \ll \theta, \\ \tau_{\rm ph}^{-1} &= b_2\omega T\theta^3/\rho(\bar{s})^2 s_l^3\hbar^3 \text{ for } T \gg \theta, \end{aligned} \qquad (4)$$

where the b_i are constants, and ρ is the density of the material. Other processes which are allowed by energy and momentum conservation for phonons—the connection of a transverse thermal phonon to a transverse subthermal phonon, accompanied by the formation of a longitudinal thermal phonon; the connection of a subthermal transverse phonon to a thermal longitudinal phonon, accompanied by the formation of a transverse thermal phonon; and the inverse decay processes—can occur if all the phonons involved in the process have energies on the same order of magnitude. As a result, the corresponding reciprocal relaxation time is proportional to the fourth degree of the frequency. In other words, it contains a small factor $(\hbar\omega/T)^3$ or $(\hbar\omega/\theta)^3$ in comparison with the Landau-Rumer expression, (4). Such relaxation processes can accordingly be ignored.

Landau–Rumer processes make it possible to find an estimate of the average phonon relaxation time. We find $\tau_{\rm ph}$ by setting the phonon energy equal to T and θ, respectively, in (4). Phonon–phonon scattering processes are always proportional to the small parameter of the anharmonic interaction, $\theta^4/\rho(\bar{s})^5\hbar^3 \ll 1$. Using (2) and (4), we verify that the integrand in (1) has a maximum at the frequency at which the impurity scattering becomes comparable to the phonon–phonon scattering:

$$\omega_m = T[\tau_I(T)/\tau_{\rm ph}(T)]^{1/3} \quad \text{or} \quad \omega_m = \theta[\tau_I(\theta)/\tau_{\rm ph}(\theta)]^{1/3}.$$

These frequencies dominate the integral (1), determining the temperature dependence and concentration dependence of the thermal conductivity:[12]

$$\varkappa^t = \frac{3^{1/2} s_t^2 s_l \theta^2 \rho^{1/3}}{27\pi b_1^{1/3} A^{2/3} T^{4/3} \hbar (\bar{s})^{7/3}} \propto C^{-2/3} T^{-4/3} \quad \text{for} \quad T \ll \theta, \qquad (5a)$$

$$\varkappa^t = \frac{3^{1/2} s_t^2 s_l \theta \rho^{1/3}}{27\pi b_2^{1/3} A^{2/3} T^{1/3} \hbar (\bar{s})^{7/3}} \propto C^{-2/3} T^{-1/3} \quad \text{for} \quad T \gg \theta. \qquad (5b)$$

It is a more complex matter to determine how the longitudinal phonon branch contributes to the thermal conductivity. Analysis of all the processes listed above in which a low-frequency longitudinal phonon is involved shows that these processes are possible only for phonons whose energies are comparable in order of magnitude. As a result, the reciprocal phonon relaxation time is proportional to the fourth power of the frequency. The frequency dependence of the phonon-phonon scattering is thus just as strong as that of the impurity scattering in the model of an isotropic medium, and it cannot prevent the divergence of integral (1). We are obliged to go beyond the scope of the simple model of an isotropic medium and to examine more-complex phonon-scattering processes, which are closer to the situation in real crystals: Herring processes and Simons processes.

3. Herring processes incorporate the difference between the symmetry of real crystals and isotropic symmetry, so degeneracy of two transverse branches is possible. Near the lines of this degeneracy, the energy and momentum conservation laws allow a low-frequency longitudinal phonon to attach to a thermal phonon of one of the degenerate transverse branches, in a process accompanied by the formation of a thermal phonon of the other degenerate transverse branch. Since the phase volume for such nearly degenerate frequencies is small, there are corresponding low-frequency factors for a longitudinal phonon in the expression for the reciprocal relaxation time:[12]

$$\tau_{\mathrm{ph,X}}^{-1}=b_{1,\mathrm{X}}\omega^m T^{5-m}/\rho(\bar{s})^2 s_t^3\hbar^{4-m} \qquad \text{for} \qquad T\ll\theta, \tag{6a}$$

$$\tau_{\mathrm{ph,X}}^{-1}=b_{2,\mathrm{X}}\omega^m T\theta^{4-m}/\rho(\bar{s})^2 s_t^3\hbar^{4-m} \qquad \text{for} \qquad T\gg\theta. \tag{6b}$$

The exponent m differs for crystals of different symmetry, taking on values from 2 to 4. For bismuth it is 3. This value tells us that Herring processes nevertheless have a frequency dependence weaker than that of impurity scattering.

4. We turn now to the connection of a longitudinal low-frequency phonon to a thermal longitudinal phonon, in a process accompanied by the formation of a thermal longitudinal phonon. For an isotropic medium, the negative dispersion of the phonon frequency rules out satisfaction of energy and momentum conservation in a process of this sort. Simons incorporated the finite lifetime of a thermal phonon due to processes by which it is scattered. This effect "blurs" the selection rules imposed by the conservation laws. Since the dispersion of the phonon frequency prevents such blurring, the relative weights of these factors determine the form of the Simons relaxation time:[13]

$$\tau_{\mathrm{ph},C}^{-1}=b_{11,\mathrm{C}}\omega T^4/\rho(\bar{s})^2 s_l^3\hbar^3 \qquad \text{for} \qquad T\ll\theta,$$
$$\tau_I^{-1}(T)\ll\omega\ll\tau_I^{-1}(T)\beta^{-1}(\theta/T)^2; \tag{7a}$$

$$\tau_{\mathrm{ph},C}^{-1}=b_{12,\mathrm{C}}AT^6/\rho(\bar{s})^2 s_l^3\theta\hbar^4 \qquad \text{for} \qquad T\ll\theta,$$
$$\omega\gg\tau_I^{-1}(T)\beta^{-1}(\theta/T)^2; \tag{7b}$$

$$\tau_{\mathrm{ph},C}^{-1}=b_{21,\mathrm{C}}\omega T\theta^3/\rho(\bar{s})^2 s_l^3\hbar^3 \qquad \text{for} \qquad T\gg\theta,$$
$$\tau_I^{-1}(\theta)\ll\omega\ll\tau_I^{-1}(\theta)\beta^{-1}, \tag{7c}$$

$$\tau_{\mathrm{ph},C}^{-1}=b_{22,\mathrm{C}}AT\theta^4/\rho(\bar{s})^2 s_l^3\hbar^4 \quad \text{for} \quad T\gg\theta,$$
$$\omega\gg\tau_I^{-1}(\theta)\beta^{-1}. \tag{7d}$$

The constant β determines the dispersion of the longitudinal frequency and has a value $\sim 1/3$. We see that (7a) and (7c) correspond to conditions in which the lifetime of a longitudinal thermal phonon is such that the selection rule due to the frequency dispersion is no longer in force. In this case the intensity of the Simons process is on the order of that of Landau–Rumer processes. Consequently, the intensity of Simons processes is determined exclusively by the phonon-phonon interaction. It is natural to compare these intensities with the intensity of the Herring processes (6a) and (6b), which are also determined by the phonon-phonon interaction alone. It turns out that these Simons processes are always stronger than the Herring processes, since the intensity of the latter contains a relatively small factor $(\hbar\omega/T)^{m-1}$ or $(\hbar\omega/\theta)^{m-1}$. Equations (7b) and (7d) and Eqs. (7a) and (7c) correspond to the opposite relation between the lifetime and the frequency dispersion of a longitudinal thermal phonon. In this case the intensity of Simons processes is determined by higher-order perturbation theory in the phonon-phonon and phonon-impurity interactions.

Substituting (6) and (7) into (1), we find the following behavior: at low temperatures, $T\ll\theta$,

$$\varkappa_{\mathrm{ph},C}^{1}=\frac{3^{1/2}s_l^3\theta^2\rho^{1/3}}{27\pi b_{11,\mathrm{C}}^{1/3}A^{2/3}T^{4/3}\hbar(\bar{s})^{7/3}}\propto C^{-2/3}T^{-4/3},$$
$$1\ll\theta^4/A^{4/3}T^{8/3}[\rho(\bar{s})^2]^{1/3}\hbar s_l\ll\beta^{-1}(\theta/T)^2; \tag{8a}$$

$$\varkappa_{\mathrm{ph},C}^{1}=\frac{2^{1/2}s_l^{11/4}\theta^{5/2}\rho^{1/4}}{24\pi b_{12,\mathrm{C}}^{1/4}AT^{3/2}\hbar^{5/4}(\bar{s})^{5/2}}\propto C^{-1}T^{-3/2},$$
$$\theta^4/A^{4/3}T^{8/3}[\rho(\bar{s})^2]^{1/3}\hbar s_l\gg\beta^{-4/3}(\theta/T)^2, \tag{8b}$$
$$\hbar^{9/4}A[\rho(\bar{s})^2]^{3/4}s_l^{9/4}/\theta^{5/2}T^{1/2}\gg 1;$$

$$\varkappa_{\mathrm{ph,X}}^{1}=\frac{\rho s_l^2 s_t^3}{6\pi^2 b_{1,\mathrm{X}}\bar{s}T^2}\ln\frac{T^{2/3}\theta^{10/3}}{\rho(\bar{s})^2 s_t^3\hbar^3 A^{4/3}}\propto T^{-2}\ln(DT^{2/3}C^{-4/3}),$$
$$\hbar^{9/4}A[\rho(\bar{s})^2]^{3/4}s_l^{9/4}/\theta^{5/2}T^{1/2}\ll 1, \tag{8c}$$

at high temperatures, $T\gg\theta$,

$$\varkappa_{\mathrm{ph},C}^{1}=\frac{3^{1/2}s_l^3\theta\rho^{1/3}}{27\pi b_{21,\mathrm{C}}^{1/3}A^{2/3}T^{1/3}\hbar(\bar{s})^{7/3}}\propto C^{-2/3}T^{-1/3},$$
$$1\ll T^{1/3}\theta/A^{4/3}\hbar[\rho(\bar{s})^2]^{1/3}s_l\ll\beta^{-1}; \tag{9a}$$

$$\varkappa_{\mathrm{ph},C}^{1}=\frac{2^{1/2}s_l^{11/4}\theta^{5/4}\rho^{1/4}}{24\pi b_{22,\mathrm{C}}^{1/4}AT^{1/4}\hbar^{5/4}(\bar{s})^{5/2}}\propto C^{-1}T^{-1/4},$$
$$T^{1/3}\theta/A^{4/3}\hbar[\rho(\bar{s})^2]^{1/3}s_l\gg\beta^{-4/3}, \tag{9b}$$
$$A(\theta/T)^{3/4}[\rho(\bar{s})^2]^{3/4}s_l^{9/4}\hbar^{9/4}\theta^{-3}\gg 1;$$

$$\varkappa_{\mathrm{ph},C}^{1}=\frac{\rho s_l^2 s_t^3}{6\pi^2 b_{2,\mathrm{X}}(\bar{s})T\theta}\ln\frac{T\theta^3}{A^{4/3}\rho(\bar{s})^2 s_t^3\hbar^3}\propto T^{-1}\ln(BTC^{-4/3}),$$
$$A(\theta/T)^{3/4}[\rho(\bar{s})^2]^{3/4}s_l^{9/4}\hbar^{9/4}\theta^{-3}\ll 1. \tag{9c}$$

Inequalities (8b) and (9b) can be compatible, because of the small anharmonic-interaction parameter, which we mentioned earlier. As expected, the behavior in (8a) and (9a) is the same as in (5), but the conditions for applicability are severe.

The temperature dependence and concentration dependence of the thermal conductivity of insulators at low temperatures were classified in Ref. 14. Unfortunately, one of the results in (8a) was not cited, although that result turns out to be the most important one in a comparison of theory and experiment.

We would also like to present the dependence which probably arises at temperatures on the order of the Debye temperature. This behavior was seen by one of the present authors in a previous study,[15] where it was shown that this dependence is determined by a rather involved hierarchy of phonon-phonon and phonon-impurity scattering mechanisms, involving both thermal and subthermal phonons. The final expression is

$$\varkappa_{\mathrm{ph}}=b_3\frac{\theta^{2/3}\rho^{4/9}(\bar{s})^{11/9}}{A^{2/9}T^{4/9}\hbar^{2/3}}\propto C^{-2/9}T^{-4/9}, \quad \theta^4/\rho(\bar{s})^5A^4\hbar^3\ll 1. \tag{10}$$

The fractional dependence on the temperature and on the concentration arises here because the thermal conductivity is dominated by the group of subthermal phonons which have the longest mean free path under the given conditions. This group of phonons contributes little to the specific heat of the crystal, so one cannot accept the idea of singling out thermal phonons as a separate factor in the thermal conductivity,[14] under the assumption that the factor which remains is an effective mean free path. As we will see below, what serves as the effective mean free path is the longest one. If we use it instead, we could determine the specific heat of the effective group of phonons. All these circumstances complicate efforts to compare the thermal conductivity of a dirty insulator with a description of the thermal conductivity in a clean one, in which thermal phonons dominate the situation in nearly all cases.

5. If the smallest dimension of the sample is comparable to the mean free path for the frequency ω_m which dominates the integral (1), the thermal conductivity begins to depend on the size of the sample. A very simple estimate is found by adding a term s_i/d to expression (2), i.e., by incorporating boundary scattering by introducing an additional relaxation time. If this time becomes shorter than $\tau_{\text{ph}}(\omega_m)$, the thermal conductivity is determined exclusively by impurity scattering and boundary scattering, and it is totally independent of the temperature:[12]

$$\varkappa_{\text{ph}} = \frac{2^{1/2} d^{1/4} \theta^{9/4}}{24\pi A^{3/4} (\bar{s})^3 \hbar^{9/4}} \sum_i s_i^{7/4} \propto d^{1/4} C^{-3/4}. \tag{11}$$

This is the behavior of the thermal conductivity as a function of the dimensions at the maximum of the temperature dependence in a dirty insulator.

However, even when the dimensions of the sample are greater than the mean free path we incorporate boundary scattering by introducing an additional relaxation time. The idea is to find the size correction to the thermal conductivity given by (5), (8a), and (8b):

$$\Delta\varkappa \approx -\sum_i \frac{s_i^3}{d} \frac{4\pi}{3} \int_0^{\theta/\hbar} \frac{d\omega}{(2\pi)^3} \rho(\omega) \tau_i^2 \partial N_{0i}/\partial T, \tag{12}$$

$$\Delta\varkappa = -\frac{2 \cdot 3^{1/2} s_l^8 (\bar{s})^{1/3} \rho^{5/3} \theta \hbar^4}{81\pi d T^{20/3} A^{1/3} b_{11,\,\text{C}}^{5/3}} \propto -d^{-1} C^{-1/3} T^{-20/3}, \tag{12a}$$

$$\Delta\varkappa = -\frac{2^{1/2} s_l^{27/4} \rho^{5/4} \hbar^{11/4} \theta^{7/2}}{96\pi d T^{15/2} A^2 (\bar{s})^{1/2} b_{12,\,\text{C}}^{5/4}} \propto -d^{-1} C^{-2}\, T^{-15/2}. \tag{12b}$$

Incorporating scattering at the boundary by introducing an additional relaxation time is not totally rigorous. A correct analysis of the dependence on the dimensions of the sample should be based on the solution of the kinetic equation for the phonon gas incorporating the boundedness of the crystal. In an effort to test (11) and (12), we have carried out a solution of this sort. We will not reproduce it here because it is lengthy and opaque, but we will present the results. In solving the equation, one should impose a boundary condition on the reflection of phonons at the boundary of the sample. If the reflection is specular, there will be no dissipation of momentum, and there will be no relaxation of the phonon distribution function. A rigorous analysis under this boundary condition in fact shows that the entire dependence on the dimensions of the sample drops out of the solution. In other words, if a behavior like that in (11) and (12) is to be obtained it is necessary to introduce some degree of diffuse reflection in the law describing the reflection of phonons at the boundary.

We carried out the analysis for regions of two types: a very long cylinder along which a temperature gradient is applied and the region between two infinite plates, with the temperature gradient parallel to the plane of the plates. In general, the description depends strongly on the geometry of the sample. The rigorous analysis completely confirms the behavior in (11) near the temperature maximum. This behavior arises regardless of the geometry of the sample.

For the behavior (12), the situation is different. It turns out that the expression for $\Delta\varkappa$ contains terms of the form (12), which appear with both positive and negative coefficients. Since the general expression is rather complicated, we have been unable to prove that these terms cancel out completely, but it is possible that they cancel out to a substantial extent. It is difficult to determine the temperature dependence of the correction $\Delta\varkappa$, but one might expect it to be determined by the contribution from the range of energies on the order of thermal energies to the integral in (12). In deriving (12a) and (12b), we ignored those energies, assuming that the corresponding contribution was parametrically small in comparison with the contribution from the low-energy region. However, since the result which was obtained by solving the kinetic equation indicates a sharp decrease in the low-energy contribution to the integral, we believe that the thermal-energy contribution is the leading contribution. If so, the expression for the correction to the thermal conductivity becomes

$$\Delta\varkappa = -\frac{b_4 s_l^3 \theta^6}{d (\bar{s})^3 A^2 \hbar T^5} \propto -d^{-1} C^{-2} T^{-5}. \tag{13}$$

DISCUSSION OF EXPERIMENTAL RESULTS

Let us compare the experimental data on the behavior of the phonon thermal conductivity as a function of the temperature (for $T < \theta$ and for $T > \theta$) and as a function of the concentration of the isovalent antimony impurity (up to 60 at. %) in the bismuth (Figs. 1 and 2), on the one hand, with the theoretical results presented above. That theory incorporates the effect of defects on the thermal conductivity of an insulator. Experimentally, the bismuth thermal conductivity is observed to behave in a variety of ways, from the well-known temperature dependence for a clean insulator to the asymptotic expressions for a dirty insulator found from the theory presented above. Those asymptotic expressions can be interpreted reliably.

The temperature dependence and the concentration dependence observed here (for the first time) for the thermal conductivity of $\text{Bi}_{1-x}\text{Sb}_x$ $(0.08 < x \leqslant 0.16)$ alloys, i.e., $\varkappa_{\text{ph}}(T,C) \propto C^{-2/3} T^{-4/3}$ at low temperatures $(T_M < T < \theta)$, can be described well by the theoretical expressions (5a) and (8a). At high temperatures $(T > \theta)$, the behavior $\varkappa_{\text{ph}}(T,C) \propto C^{-2/3} T^{-1/3}$ again agrees with the theoretical expressions, in this case (5b) and (9b). Those expressions were derived for the case of a composite mechanism for phonon scattering, involving scattering by both impurities and phonons. Simons scattering processes are predominant for the case of scattering by phonons. For the alloy $\text{Bi}_{1-x}\text{Sb}_x$ $(0.03 < x < 0.08)$, with a lower antimony concentration, the observed temperature and concentration dependence, i.e.,

$\varkappa_{ph}(C,T) \propto C^{-1/2}T^{-3/2}$ at low temperatures and $\varkappa_{ph}(C,T) \propto C^{-1/2}T^{-1/2}$ at high temperatures, is a transitional dependence between the exponential dependence $\varkappa_{ph}(T)$ in pure Bi and the power-law dependence $\varkappa_{ph}(C,T)$ in $Bi_{1-x}Sb_x$ $(0.08 < x \leqslant 0.16)$ alloys. This transitional behavior of $\varkappa_{ph}(C,T)$ for the alloy $Bi_{1-x}Sb_x$ $(0.03 < x < 0.08)$ cannot be described satisfactorily by the theoretical expressions (8b) and (9b). Although the temperature dependence of the thermal conductivity for the alloys at $T < \theta$ is the same as that described by (8b), the dependence on the defect concentration is different.

We mentioned earlier that the theory agrees well with the experimental data on the temperature and concentration dependence of the thermal conductivity for alloys $Bi_{1-x}Sb_x$ $(0.08 < x \leqslant 0.16)$. We should also note that for alloys of this composition there is a good agreement between experiment and theory in the analysis of the behavior of the maximum of the phonon thermal conductivity as a function of the defect concentration and the transverse dimensions of the sample [see (11)], $\varkappa_{ph}(C,d) \propto d^{1/4}C^{-3/4}$.

In the alloys, as in pure bismuth, there is a maximum on the temperature dependence of the phonon thermal conductivity (Fig. 1). In bismuth, the mean free path of the thermal phonons for $T < T_M$ is limited by the transverse dimensions of the sample, so we have $\varkappa_{ph}(T) \propto C(T) \propto T^3$. In the alloy, we should again obtain this limiting case, in which the heat is transferred primarily by thermal phonons, as the temperature is lowered. For the thermal phonons, scattering by the surface of the sample becomes dominant, and the scattering by the impurity becomes fairly weak. In the alloys, however, this change should occur only at very low temperatures ($T \approx 0.1$ K). For this reason, the decrease in the phonon thermal conductivity in the alloys for $T < T_M$ is naturally linked with an approach to this limiting behavior. The transition to this behavior occurs more slowly, the higher the antimony concentration in the alloy.

Going back to the size effect, we note that theoretical expression (13) describes a small correction far from the temperature of the maximum ($T > T_M$). At the maximum, $T \approx T_M$, the thermal conductivity depends very strongly on the dimension d according to (11). Experimentally, on the other hand, the correction to the thermal conductivity was measured at intermediate temperatures, $T/T_M \approx 2$–3 (Fig. 3). Although $\Delta\varkappa$ is only a small part of the total thermal conductivity in this region, we cannot guarantee that the asymptotic expression (13) will be applicable. However, the experimental value of $\Delta\varkappa$ (Fig. 4) is comparable to (13) in terms of the qualitative behavior as a function of the size and temperature and also in terms of sign.

CONCLUSION

This study of the phonon thermal conductivity of bismuth-based alloys (Bi–Sb) as a function of the temperature and the defect (Sb) concentration turned out to be successful only because the original matrix of the alloy—the bismuth—consists of only a single isotope. There is no isotopic scattering of phonons in pure Bi, but we do see it in the Bi–Sb alloys. It strengthens with increasing Sb concentration.

A dependence of the phonon thermal conductivity on the temperature and the Sb concentration has been observed experimentally for the first time in $Bi_{1-x}Sb_x$ $(0.08 < x \leqslant 0.16)$ alloys: $\varkappa_{ph}(C,T) \propto C^{-2/3}T^{-4/3}$ for $T_M < T < \theta$ and $\varkappa_{ph}(C,T) \propto C^{-2/3}T^{-1/3}$ for $T > \theta$. This behavior of the thermal conductivity can explained theoretically on the basis of a mixed mechanism for phonon scattering in a dirty insulator—scattering by both defects and phonons, but with Simons processes dominating the phonon–phonon interaction.

On the basis of this theoretical analysis of the thermal conductivity in dirty insulators and of the experimental data on the phonon thermal conductivity of $Bi_{1-x}Sb_x$ $(0 < x \leqslant 0.16)$ alloys we can conclude that Simons processes are predominant in the phonon-phonon interaction at high Sb concentrations ($x > 0.08$). Only at lower Sb concentrations ($x < 0.03$) could Herring processes, with a thermal-conductivity behavior as in (8c) and (9c), become dominant in the phonon-phonon interaction. Further research will be required to explain this fact.

An important result of this study of the phonon thermal conductivity of $Bi_{1-x}Sb_x$ alloys for $T \geqslant \theta$ is the observation of a threshold Sb concentration ($x > 0.003$), at which the thermal conductivity starts to become lower than the $\varkappa_{ph}(T) \propto T^{-1}$ for pure bismuth. As a result, there is a temperature dependence $\varkappa_{ph}(T) \propto T^{-n}$ $(n < 1)$. Near the temperature of the maximum in the phonon thermal conductivity of the Bi–Sb alloys, on the other hand, there is no threshold Sb concentration, and the magnitude of the thermal conductivity decreases at an arbitrarily low concentration of defects.

According to the experimental data on the phonon thermal conductivity of the $Bi_{1-x}Sb_x$ $(0 < x \leqslant 0.16)$ alloys, the thermal conductivity reaches a maximum near $T = 4$ K, but this maximum becomes rounded as the Sb concentration increases (Fig. 1). A further theoretical analysis will be required to explain this behavior of the maximum of the phonon thermal conductivity of the alloys.

A point we would particularly like to stress is that the size effect has been taken into account in this study of the temperature dependence of the phonon thermal conductivity in Bi–Sb alloys. This effect may be manifested at low temperatures $T > T_M$. The dependence of the phonon thermal conductivity at the maximum on the transverse dimensions of the sample and on the defect concentration which has been found, $\varkappa_{ph}(C,d) \propto C^{-3/4}d^{1/4}$, in contrast with the $\varkappa_{ph}(d) \propto d$ for pure bismuth, can serve as confirmation that phonons are scattered by defects in alloys with a sufficiently high antimony content.

We wish to thank N. A. Rodionov and V. I. Pol'shin for furnishing the Bi–Sb single crystals which were grown.

[1] J.-P. Issi and J. Hermans, in *Proceedings, XV International Conference on Thermal Conductivity*, Ottawa, 1977, p. 63.

[2] I. Ya. Korenblit, M. E. Kuznetsov, V. M. Muzhdaba, and S. S. Shalyt, Zh. Eksp. Teor. Fiz. **57**, 1867 (1969) [Sov. Phys. JETP **30**, 1009 (1970)].

[3] V. N. Kopylov and L. P. Mezhov-Deglin, Zh. Eksp. Teor. Fiz. **65**, 720 (1973) [Sov. Phys. JETP **38**, 357 (1974)]; L. P. Mezhov-Deglin, V. N. Kopylov, and É. S. Medvedev, Zh. Eksp. Teor. Fiz. **67**, 1123 (1974) [Sov. Phys. JETP **40**, 557 (1975)].

[4] M. E. Kuznetsov, V. S. Oskotskiĭ, V. I. Pol'shin, and S. S. Shalyt, Zh. Eksp. Teor. Fiz. **57**, 1112 (1969) [Sov. Phys. JETP **30**, 607 (1970)].

[5] V. Narayanamurti and R. C. Dines, Phys. Rev. Lett. **28**, 1461 (1972).

[6] T. Yazaki, J. Phys. Soc. Jpn. **25**, 1054 (1968).

[7] T. K. Dey and K. D. Chaudhuri, J. Low Temp. Phys. **23**, 419 (1976).

[8] P. P. Bodyul, M. P. Boĭko, and N. A. Red'ko, Fiz. Tverd. Tela (Leningrad) **28**, 3182 (1986) [Sov. Phys. Solid State **28**, 1793 (1986)].

[9] N. A. Red'ko, Pis'ma Zh. Tekh. Fiz. **16**(22), 52 (1990) [Sov. Tech. Phys. Lett. **16**, 868 (1990)].

[10] H. Berger, B. Christ, and J. Troschke, Cryst. Res. Tech. **17**, 1233 (1982).

[11] N. B. Brandt, R. Germann, G. I. Golysheva *et al.*, Zh. Eksp. Teor. Fiz. **83**, 2152 (1982) [Sov. Phys. JETP **56**, 1247 (1982)]; G. A. Mironova, M. V. Sudakova, and Ya. G. Ponomarev, Fiz. Tverd. Tela (Leningrad) **22**, 3628 (1980) [Sov. Phys. Solid State **22**, 2124 (1980)].

[12] V. L. Gurevich, *Transport in Phonon Systems*, Nauka, Moscow, 1980, p. 400 (North-Holland, Amsterdam, 1986).

[13] L. É. Gurevich, Fiz. Tverd. Tela (Leningrad) **9**, 526 (1967) [Sov. Phys. Solid State **9**, 401 (1967)].

[14] R. N. Gurzhi and A. O. Maksimov, Fiz. Nizk. Temp. **3**, 346 (1977) [Sov. J. Low Temp. Phys. **3**, 171 (1977)].

[15] V. D. Kagan, Fiz. Tverd. Tela (Leningrad) **23**, 1551 (1981) [Sov. Phys. Solid State **23**, 909 (1981)].

Translated by D. Parsons